Journal Name

ARTICLE TYPE

Cite this: DOI: 10.1039/xxxxxxxxxx

The dp type π-bond and chiral charge density wave in $1T$-$TiSe_2$

Guo-Jiun Shu,[a,b,c,d] Sz-Chian Liou,[e] Chih-Kai Lin,[a] Michitoshi Hayashi,[a] and Fang-Cheng Chou*[a,d,f,g]

Received Date
Accepted Date

DOI: 10.1039/xxxxxxxxxx

www.rsc.org/journalname

Based on atomic electronic configuration and Ti-Se coordination, a valence bond model for the layered transition metal dichalcogenide (TMDC) $1T$-$TiSe_2$ is proposed. $1T$-$TiSe_2$ is viewed being composed of edge-sharing $TiSe_4$-plaquettes as $TiSe_2$-ribbon chains in each layer via a directional valence shell electron distribution as chemical bonds, in contrast to the conventional layer view of face-sharing $TiSe_6$-octahedra. The four valence electrons per Ti in hybridized dsp^2-orbitals of square coordination form σ-bonds with the four nearest neighbor Se atoms in the chain. The electrons in the lone pair of the Se-$4p_z$ orbital are proposed to form a dp type π-bond via side-to-side orbital overlap with the empty Ti-$3d_{xz}/3d_{yz}$ orbitals within each chain, which is positively supported by quantum chemistry calculations. A study of electron energy loss spectroscopy (EELS) with transmission electron microscopy (TEM) for $1T$-$TiSe_2$ is presented to show an energy loss near $\sim$7 and $\sim$20 eV, which confirms the existence of collective plasmon oscillations with the predicted effective electron numbers for the π- and $(\pi+\sigma)$-bond electrons, respectively.

1 Introduction

Following the heavily investigated graphene as a prototype 2D monoatomic layered compound,[1] the great potential for device applications of few layer TMDC compounds has led a new direction in the applied research of 2D materials.[2,3] Among the many varieties of layered TMDC compounds with a composition of MX_2 (M=transition metal, X=S, Se, Te), one finds that multiple stacking forms layers of octahedral-coordinated (T-type) or trigonal prismatic-coordinated (H-type) M-X units. For example, the most common $2H$-type (two layers of edge-shared MX_6 trigonal prismatic per unit cell) or $3R$-type (three layers of edge-shared MX_6 octahedra per unit cell) depends on the M-X element combination and growth condition.[4] The latest development of topological materials has generated interest in revisiting layered TMDC compounds;[5] for example, the subtle symmetry change of polymorphic $MoTe_2$ in 2D leads to a change in its physical character from $2H$-type semiconductor to $1T'$-type, and becomes a Weyl semimetal of T_d-type at low temperature.[6,7] Among the rich varieties of TMDC compounds, $TiSe_2$ is unique for having only one $1T$-type structure, with each tri-atomic layer composed of edge-sharing $TiSe_6$-octahedra.[8]

Despite the simple layered structure, $1T$-$TiSe_2$ has been intensely studied since the 70's due to many inconsistent observations and conflicting interpretations, including the origin of the observed unconventional 2a*2a*2c charge density wave (CDW) without Fermi surface nesting, the classification of being a semiconductor or semimetal, and the varieties of vacancy defects.[9–11] Here, based on the integrated studies of electronic configuration

[a] Center for Condensed Matter Sciences, National Taiwan University, Taipei 10617, Taiwan
[b] Department of Materials and Mineral Resources Engineering, National Taipei University of Technology, Taipei 10608, Taiwan
[c] Institute of Mineral Resources Engineering, National Taipei University of Technology, Taipei 10608, Taiwan
[d] Taiwan Consortium of Emergent Crystalline Materials, Ministry of Science and Technology, Taipei 10622, Taiwan
[e] AIM Lab, Nano Center, University of Maryland, College Park, MD 20742, U.S.A.
[f] National Synchrotron Radiation Research Center, Hsinchu 30076, Taiwan
[g] Center of Atomic Initiative for New Materials, National Taiwan University, Taipei 10617, Taiwan. Fax: +886-2-23655404; Tel: +886-2-33665254; E-mail: fcchou@ntu.edu.tw

and crystal symmetry, we re-visit the electronic structure of $1T$-$TiSe_2$ following a newly proposed valence bond model that has been successfully applied to interpret experimental data obtained for Na_xCoO_2 and Bi_2Se_3.[12,13] Based on the newly proposed valence bond model, each layer of $1T$-$TiSe_2$ is viewed as being composed of $TiSe_2$-ribbon chains of conserved valence electron pairing, instead of the conventional view of edge-sharing $TiSe_6$-octahedra. Most importantly, a conjugated dp type π-bond system can be identified, which is similar to the pp type π-bond found in graphene and the topological crystalline insulator $Pb_{1-x}Sn_xSe$.[14] The proposed dp type π-bond model is positively supported by quantum chemistry calculations. The EELS spectrum is presented to support the proposed valence bond model via the identification of energy absorption due to collective plasma oscillations of the π- and σ-bond electrons. In particular, the effective number of electrons per formula unit is found to be in excellent quantitative agreement with the valence bond model prediction.

A band picture for a material in energy-momentum space with E(**k**) dispersion relation is a common tool used for describing condensed matter having electrons in a periodic potential, which relies heavily on the 3D crystalline symmetry probed by diffraction techniques. While band filling under the assumptions of a periodic electron distribution must closely follow the atomic symmetry, many exceptions were found in between the prototypical ionic insulator and the Fermi liquid metal. The failure of a simple band theory that predicts transition metal oxides should show a half-filled band and be an insulator, instead of a metal, has been resolved by the introduction of a Mott gap U originated from the Coulomb repulsion, which has been categorized as a strongly correlated electron system.[15] The latest development of topological materials has introduced additional complications involving strong spin-orbit coupling induced band inversion leading to unexpected surface conduction, which has been classified as a material system having symmetry-protected topological orders.[5,16]

We believe that describing the band structure of a quasi-2D vdW material using its 3D crystalline symmetry could lead to erroneous interpretation for the mono-atomic graphene, to the $1T$-$TiSe_2$ of tri-atomic thickness per layer, and to the topological insulator Bi_2Se_3 of quintuple-atomic thickness per layer.[13] Although these layered materials can be perfectly described with a 3D crystalline symmetry, electrons across the vdW gap do not have an exchange interaction but couple via the Coulomb interaction as instantaneous electric dipoles. In this study, we have demonstrated that the quasi-2D planes in $1T$-$TiSe_2$ should be chemically viewed as 1D $TiSe_2$-ribbon chains, which reveals a subtle discrepancy between the actual Bragg planes responsible for the diffraction phenomenon and the lattice planes defined by the L-point in the 1st BZ. As a result, the band picture mapped with ARPES experiments should be re-interpreted by considering the symmetry of the bound electrons in the chemical bonds.

2 Experimental and calculation details

Single crystal $1T$-$TiSe_{2-\delta}$ with $\delta\sim0.12$ having the most pronounced 2a*2a*2c CDW resistivity peak near $\sim$200 K has been adjusted via vacuum sealed annealing, as fully described previously.[17] Additional low temperature annealing for the as-grown single crystal samples was performed by sealing the as-grown crystals in Se-rich and evacuated quartz tubing at 250°C for more than six months, which enables the refilling of Se into the vacancy sites for reaching a stoichiometry of $\delta\sim0$.

For the TEM specimen, single crystal $1T$-$TiSe_2$ with a cleavable ab-plane was exfoliated by repeated mechanical cleaving using adhesive tape until it was thinned to a thickness of approximately 50 nm and then was transferred to the TEM grid. The electron energy loss spectrum for $1T$-$TiSe_2$ was measured using a JEOL 2100F field-emission gun operated at 200 kV, which is equipped with a Gatan image filter (model Tridiem 863). The scanning TEM (STEM) mode was performed with a probe convergent semi-angle of $\sim$10 mrad of energy resolution $\sim$0.8 eV.

Quantum chemistry calculations were carried out with density functional theory (DFT) methods using a B3LYP functional and 6-31G(d) basis set implanted in the Gaussian 09 computational package. First, a quasi-2D single layer $1T$-$TiSe_2$ model cluster was constructed, and then, a quasi-1D $TiSe_2$-ribbon structure was sliced out, which contained edge-shared plaquette units for each Ti atom that is bonded with four Se atoms in the common plane. The bonding characteristics were revealed and illustrated in a linear combination of atomic orbitals (LCAO) sense of molecular orbitals.

3 Results and Discussions

3.1 Crystal symmetry of $1T$-$TiSe_2$

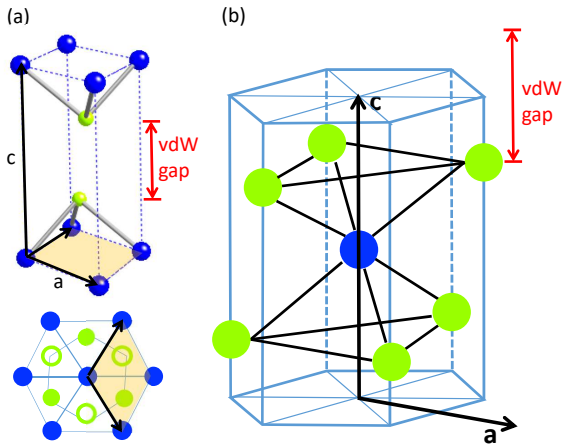

Fig. 1 The crystal structure of $1T$-$TiSe_2$ has a 3D trigonal symmetry of space group $p\bar{3}m1$ with Ti at (0, 0, 0) and Se at ($\frac{1}{3}$, $\frac{2}{3}$, $\frac{1}{4}$), as shown in (a) with a top view below. An equivalent view in the hexagonal unit is shown in (b). The existence of a vdW gap in the 3D unit cell disrupts the presumed wavefunction continuity along the c-direction.

The primitive cell of $1T$-$TiSe_2$ has a point symmetry of the trigonal space group $p\bar{3}m1$ (No. 164) with Ti at (0, 0, 0) and Se at ($\frac{1}{3}$, $\frac{2}{3}$, $\frac{1}{4}$),[17,18] which has been commonly named CdI_2-type in the conventional symmetry classification, as shown in Fig. 1(a). For the construction of the band description in **k**-space for the first BZ, it is more convenient to transform the trigonal form into an equivalent hexagonal form, as shown in Fig. 1(b). The conventional view for each $1T$-$TiSe_2$ layer is composed of edge-sharing $TiSe_6$-octahedra as a Se-Ti-Se tri-atomic layer in close packing, as

illustrated in Fig. 2(a). It must be noted that even the 3D crystal structure is fully described with the point lattice of space group $p\bar{3}m1$ using the correct atomic position assignment; the electronic structure is 2D in nature due to the existence of the vdW gap, i.e., the electronic structure is not continuous across the vdW gap. In the band structure interpretation of a vdW material, a direct real to reciprocal space conversion using the 3D crystal symmetry via Fourier transformation could be misleading as a result of a compromised assumption for the overlap of a continuous wavefunction across the vdW gap, which is in great contrast to conventional 3D materials without the vdW gap complication. We believe that for the band structure interpretation of a vdW material like $1T$-$TiSe_2$, a detailed examination of the valence electron sharing from the perspective of chemical bonding is required.

3.2 Valence bond model for $TiSe_2$-ribbon chains

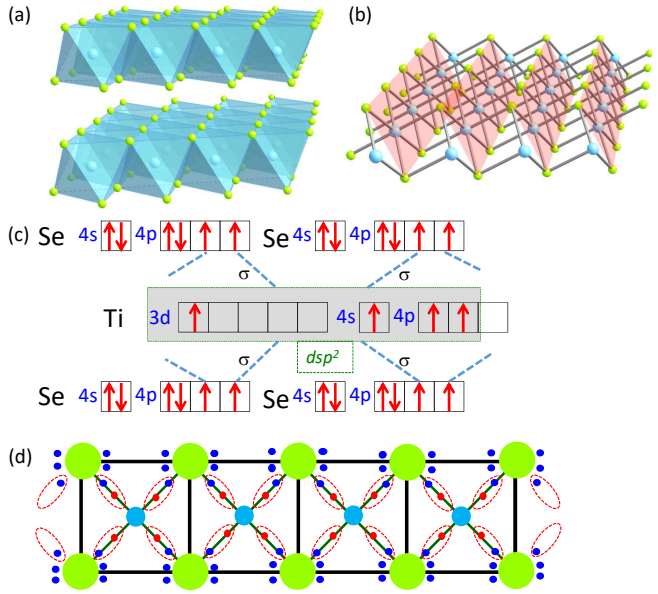

Fig. 2 (a)-(b) Under the condition that each Ti atom has only four valence electrons, the reasonable layer view of $1T$-$TiSe_2$ is based on a set of tilted $TiSe_2$-ribbon chains, instead of a layer composed of face-sharing $TiSe_6$-octahedra. (c) Based on the atomic electron configurations of Ti ([Ar]$3d^2 4s^2$) and Se ([Ar]$3d^{10} 4s^2 4p^4$), a valence bond model is proposed for $1T$-$TiSe_2$, where all valence electrons are paired in either lone pairs or σ-bonds to reflect the octet rule as illustrated in (d).

On examining the atomic electronic configuration of Ti ([Ar]$3d^2 4s^2$), only four valence electrons are found to be available for chemical bonding. Although the conventional view of each $TiSe_2$ layer has been routinely proposed to be based on edge-sharing $TiSe_6$-octahedra, it is not feasible to assign Ti bonding with six neighboring Se atoms chemically. Based on the four-fold coordination of Ti with Se atoms within each plaquette, we propose a valence bond model for $1T$-$TiSe_2$ based on the fact that each layer is actually composed of tilted $TiSe_2$-ribbon chains, as illustrated in Fig. 2(b). The apical Se atoms in the earlier view of the $TiSe_6$-octahedron (Fig. 2(a)) actually belongs to the neighboring ribbons without direct Ti-Se covalent bonding, except that the effective apical Se atoms with weaker net charge could affect the crystal electric field (CEF) of Ti, similar to the CEF of Co ion in the CoO_2-layer of Na_xCoO_2.[12,19] The existence of 1D $TiSe_2$ chains has also been suggested by tight binding model calculations via the examination of non-zero overlap integrals for pp, dp, and dd hopping pathways.[20,21]

On counting the number of available valence electrons of Ti ([Ar]$3d^2 4s^2$) and Se ([Ar]$3d^{10} 4s^2 4p^4$) for each $TiSe_4$-plaquette in the ribbon chain, the four valence electrons per Ti could form a half-filled hybridized dsp^2 orbital with four lobes pointing towards the four neighboring Se atoms at the corners, so that two half-filled Se-$4p_x$ and Se-$4p_y$ orbitals are used to form four σ bonds with Ti, as illustrated in Fig. 2(c). Fig. 2(d) shows the electronic configuration of a $TiSe_2$-ribbon chain, where both Ti and Se atoms are stabilized with a filled valence shell, i.e., eight electrons in the valence shell per atom to reflect the octet rule for chemical bonding.

3.3 Proposed dp type π-bond formation

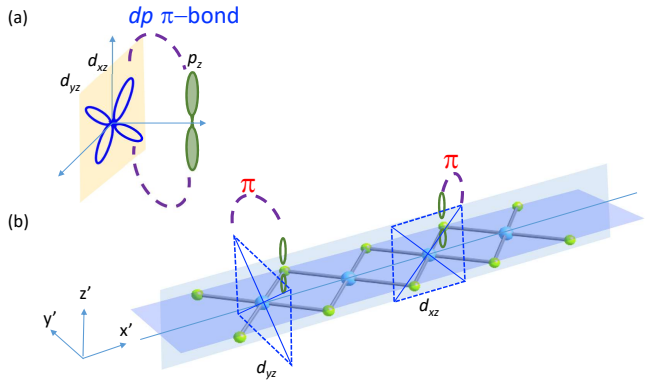

Fig. 3 (a) A dp type π-bond is proposed to be formed between the lone pair electrons of Se-$4p_z$ and the empty Ti-$3d_{xz}$ or $3d_{yz}$ orbitals via side-to-side orbital overlap, and (b) shows the two available choices for nearly orthogonal dp π-bonds via (Se)$4p_z$-(Ti)$3d_{xz}$ and (Se)$4p_z$-(Ti)$3d_{yz}$ in the $TiSe_2$-ribbon chain.

The crystal field splitting of the Ti-$3d$ orbital surrounded by Se ligands is nearly identical to that of Co surrounded by O ligands in layered Na_xCoO_2, as illustrated by its CEF of b_{1g}-a_{1g}-b_{2g}-e'_g splittings.[12] Based on the proposed valence bond model, for Ti with four valence electrons in the valence shell of $3d^2 4s^2$, only $3d_{x^2-y^2}$ is used to form a half-filled dsp^2 hybrid orbital having four lobes pointing towards the four corner Se atoms in each ribbon, which is a reasonable choice when $d_{x^2-y^2}$ has the highest energy CEF splittings before bonding.

Consider the spatial relationship of the four empty 3d orbitals (d_{z^2}, d_{xy}, d_{yz}, d_{zx}) of Ti with the filled lone pair of Se-$4p_z$ (see Fig. 2(c)-(d)), we propose that a dp type π-bond could also be formed via side-to-side orbital overlap between $4p_z$(Se)-$3d_{yz}$(Ti) or $4p_z$(Se)-$3d_{zx}$(Ti), as illustrated in Fig. 3. The side-to-side orbital overlap among half-filled neighboring d and p orbitals could lead to singlet pairing of electrons in view of the non-zero probability of wavefunction overlap. As long as a concomitant Peierls-like condensation of singlet pairing is satisfied following the Pauli exclusion principle, the π-bond formed between the empty or-

bitals of Ti-$3d_{yz}/3d_{zx}$ and the filled lone pair of Se-$4p_z$ would lead to condensation of reduced enthalpy, similar to σ-bond formation using both half-filled Ti-$3d$ and Se-$4p$ orbitals. A pp type π-bond among Pb has been previously identified in the topological crystalline insulator $Pb_{1-x}Sn_xSe$,[14] the Z_2-type topological insulator Bi_2Se_3, and the prototype 2D material of graphene,[13] which suggests a strong correlation between the existence of a conjugated π-bond system and a Dirac cone-shaped 2D band. Since all these π-bonds have been confirmed with the EELS spectra before, a similar energy absorption signature due to collective plasmonic excitation of dp type π-bond electrons is expected to be present in the EELS spectrum of $1T$-$TiSe_2$.

3.4 Evidence of σ- and π-bonds in the EELS spectrum

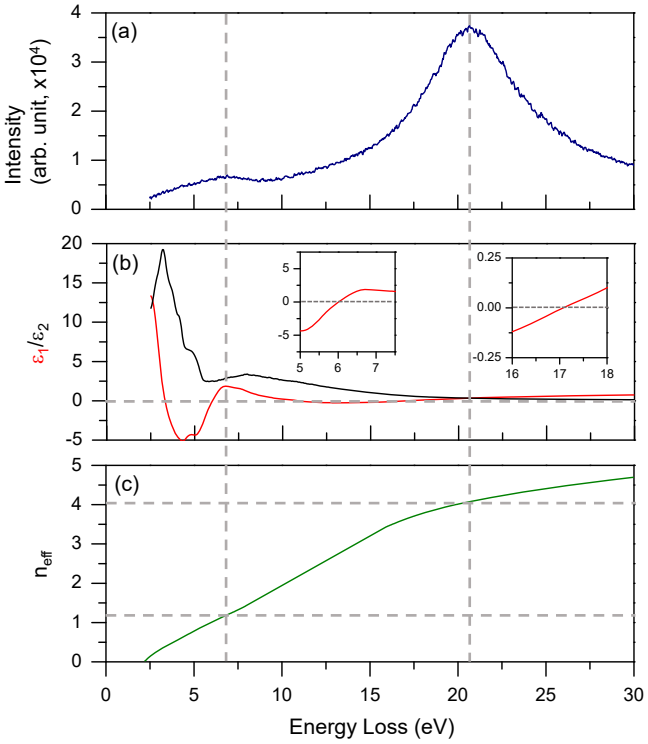

Fig. 4 EELS spectrum for the $1T$-$TiSe_2$ single crystal shows energy absorption features near 7 and 20 eV, which correspond to the collective plasmonic resonance of π and $(\pi+\sigma)$ electrons, respectively. The raw data is shown in (a), and the real (ε_1) and imaginary (ε_2) parts of the complex dielectric function are shown in (b). The insets of (b) are blown-up views of ε_1 near zero, which suggest the existence of a collective plasma oscillation (plasmon) when ε_1 passes through zero with a positive slope.[22] (c) The effective number of electrons (n_{eff}) participating in the collective resonance are calculated from ε_2 to be $n_\pi:(n_\pi+n_\sigma)\sim1.2:4$, in agreement with the valence bond model prediction.

By detecting the kinetic energy loss of an incident electron beam penetrating samples, electron energy-loss spectroscopy (EELS) has been shown to be a useful technique for exploring phenomena including intra-and inter-band transitions, as well as collective excitations with a phonon and plasmon origin. In particular, the low-loss region (energy loss $<$ 50 eV) in the EELS spectra contains useful information concerning the collective modes of the valence electron excitation, including the surface and volume plasmons.[22,23] Although the plasmonic excitation of topological insulators has been previously explored using EELS and Terahertz experiments,[24–28] we find that an intuitive understanding from a chemical bond perspective would be helpful.

The EELS spectrum for $1T$-$TiSe_2$ is shown in Fig. 4. Two main spectral features near 7 and 20 eV can be identified, with the positive slope of ε_1 across zero indicating the existence of a plasmon resonance, as indicated in the inset of Fig. 4(b).[13,14] Following the same interpretation that has been applied to the EELS spectra of graphite and Bi_2Se_3, the 7 and 20 eV features are assigned to the volume plasmons of π character and $(\pi+\sigma)$ character, respectively.[29–31] Based on the proposed valence bond model for $TiSe_2$ shown in Fig. 2, the effective number of electrons (n_{eff}) participating in the collective resonance of electrons in the π- and σ-bonds per unit (see Fig. 1) can be clearly counted. In each 2D $TiSe_2$ unit cell with Se sharing in the chain (see Fig. 2(c)-(d)), 12 valence electrons in total are distributed in the 4 σ-bonds between Ti-Se (4×2 electrons) plus two lone pairs per Se (2×2 electrons). If two dp π-bonds per 2D $TiSe_2$ unit are formed between the empty Ti($3d_{yz}$)-Se($4p_z$) lone pair and the empty Ti($3d_{zx}$)-Se($4p_z$) lone pair, it is expected that the n_{eff} for the π-bond and the $(\pi+\sigma)$-bond will be $n_\pi:(n_\pi+n_\sigma)=(2\times2):(2\times2+4\times2)=0.33$ per 2D $TiSe_2$ unit. The $n_\pi:(n_\pi+n_\sigma)$ ratio estimated from the imaginary part of the EELS spectrum (ε_2) is $\sim1.2{:}4 = 0.3$,[13] as shown in Fig. 4(c), which is in excellent agreement with the valence bond model prediction. The current EELS study results not only signify the existence of a collective oscillation of π-bond electrons in $1T$-$TiSe_2$ positively, but also offer satisfying quantitative agreement for the effective number of the π- and σ-bond electrons participating in the collective resonance, which strongly supports the validity of the proposed valence model illustrated in Figs. 2-3.

3.5 Quantum chemistry calculations for the dp type π-bond

Quantum chemistry calculations for the Ti-Se in each $TiSe_2$-ribbon of $1T$-$TiSe_2$ were performed using the probability density ($|\Psi(x,y,z)|^2$) of the corresponding dp π-bond orbital wavefunctions $\Psi_{dp\pi}(x,y,z) = N(\Psi_{4p_z} + \Psi'_{3d_{yz}/3d_{zx}})$, where Ψ_{4p_z} is the $4p_z$ orbital of Se and $\Psi'_{3d_{yz}/3d_{zx}}$ is the $3d_{yz}$ or $3d_{zx}$ orbital of Ti, as shown in Fig. 5. The Slater rule has been adopted for each atom to construct these atomic orbitals. The bonding characteristics in quasi-1D $TiSe_2$-ribbon sliced out from the $1T$-$TiSe_2$ layer are demonstrated in Fig. 5(a)-(b) based on quantum chemistry calculations. Given the $TiSe_2$-ribbon lies on the x′y′-plane and is elongated along the x′ direction, the skeleton of the ribbon is regarded as being composed of σ-bonds formed by the linear combination of in-plane Ti-dsp^2 and Se-$4p_x/4p_y$ orbitals, as suggested in Fig. 2(c) and illustrated in Fig. 5(a). The out-of-plane components of the Ti-$3d_{yz}/3d_{zx}$ and Se-$4p_z$ orbitals, on the other hand, give rise to the side-to-side dp type π-bonds, as proposed in Fig. 3(b) and illustrated in Fig. 5(b). In addition, a dp π-bond electron density contour map is shown in Fig. 5(c), where the electron density contour map for the dp type π-bond constructed by the Se-$4p_z$ and Ti-$3d_{yz}$ orbital overlap is shown on the $z'x'$-plane at $y'=r_\circ\sin(\theta/2)$ for Ti-Se having an interatomic distance of $r_\circ$=2.531Å and Se-Ti-Se bond angle of θ=91.48°. These quantum chemistry calcula-

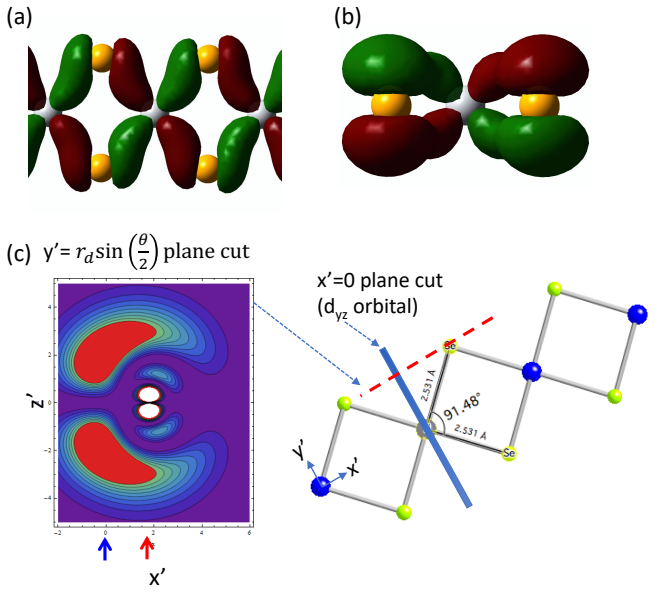

Fig. 5 The quantum chemistry calculations for the σ- and dp type π-bonds, where (a) shows the σ-bonds in the $TiSe_2$-ribbon chain plane, (b) shows the dp π-bonds above and below the $TiSe_2$-ribbon plane as viewed along the chain direction, and (c) shows the electron density contour map on the $z'x'$-plane at $y'=r_\circ \sin(\theta/2)$ for the dp π-bond constructed by the Se-4p_z and Ti-3d_{yz}, where Ti-Se atoms are separated by an interatomic distance of $r_\circ$=2.531Å and the Se-Ti-Se bond angle is θ=91.48°. The shortest distance between the Ti-d_{yz} orbital plane cut at x'=0 and the nearest neighbor Se atom is about 1.812 Å, as indicated by the two arrows at x'-axis.

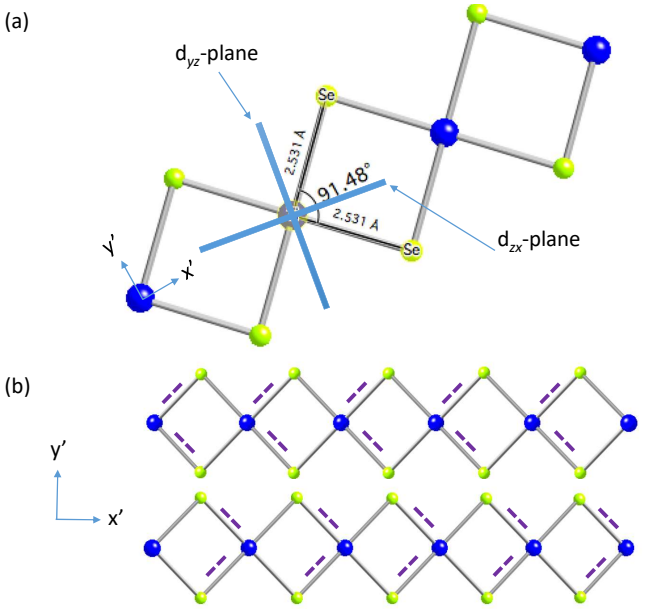

Fig. 6 (a) 1D chain condensation is implied by the slightly enlarged Se-Ti-Se bond angle of 91.48°, which most likely arises from Coulomb repulsion of electrons in the dp type π-bonds constructed by Ti-3d_{yz} and Ti-3d_{zx} with Se-4p_z on opposite sides of the $TiSe_2$-ribbon. (b) Since identical dp π-bond pairs can also be arranged in its mirror image along the chain equivalently, it is proposed that the degenerated two equivalent configurations for the π-bond pair (dashed lines) can be viewed as a conjugated system having 1D mirror symmetry protected topological orders.

tions also support the proposed dp type π-bond model which has been verified by the EELS spectroscopy.

3.6 Chain condensation in 1T-TiSe$_2$

Due to the presence of four valence electrons per Ti for four neighboring Se atoms per $TiSe_4$-plaquette, it is expected that the dsp^2 hybridized orbital of Ti should construct edge-sharing plaquettes of maintained square symmetry. However, it is interesting to note that the bond angle of S-Ti-Se along the chain is ∼91.484°, instead of the expected 90°, as shown in Fig. 6. We propose that an 1D chain condensation phenomenon may have occurred as a result of the existence of the dp type π-bond, which is reflected by the slightly enlarged Se-Ti-Se bond angle along the chain direction. Since both 3d_{yz} and 3d_{zx} orbitals of Ti are empty, both can form a dp π-bond with the lone pair of Se-4p_z. It is likely that 3d_{yz} forms a dp π-bond with one side of the Se of the $TiSe_2$-ribbon and 3d_{zx} forms a dp π-bond with Se at the opposite side, as illustrated in Fig. 6(a). The Coulomb repulsion of π-bond electrons on the opposite side would lead to a natural bond angle enlargement, as evidenced by our synchrotron X-ray diffraction verified structure refinement.[18]

In addition to the π-bond arrangement, which is responsible for bond angle enlargement, we propose that the same type of π-bond arrangement should also apply to its mirror structure along the chain direction, i.e., the two equivalent and degenerated π-bond pair arrangements may form a conjugated system under quantum fluctuation; in an alternative view, this can also be described as mirror symmetry protected topological orders, as illustrated in Fig. 6(b). In fact, this type of topological order protected by 1D mirror symmetry or translational symmetry reminds one of the similarity to the quantum spin gap systems of the Majumdar-Ghosh spin 1/2 chain and the Haldane chain of integer spin within the AKLT model description.[5,32] Considering the three equivalent chain directions per layer for 1T-TiSe$_2$, such a chemical structure is also comparable to materials containing 2D C_3 symmetry-protected topological orders, such as prototype 2D compound graphene and the surface of a topological insulator like Bi$_2$Se$_3$.[13]

3.7 Chiral CDW and charge localization near defect center

Among the many controversial topics centered on 1T-TiSe$_2$ as the prototype layered transition metal dichalcogenide, including categorization as a semiconductor or a semimetal,[10] the sample-dependent 2a*2a*2c CDW phase,[9] the varieties of surface defect types,[11] and the proposed excitonic insulator behavior for a semimetal with a CDW;[33] the existence of a chiral CDW phase as identified by Ishioka *et al.* has added additional complication.[34] We find that the proposed valence bond model can provide a natural explanation for most of these phenomena by viewing the quasi-2D tri-atomic thickness layer as chains of $TiSe_2$-ribbons.

First, in view of the 1T-TiSe$_2$ layer as $TiSe_2$-ribbon chains, as discussed above, since the σ- and dp type π-bond electrons are proposed as being aggregated near the ribbon surface like a charge stripe, it becomes natural to look for charge stripes with

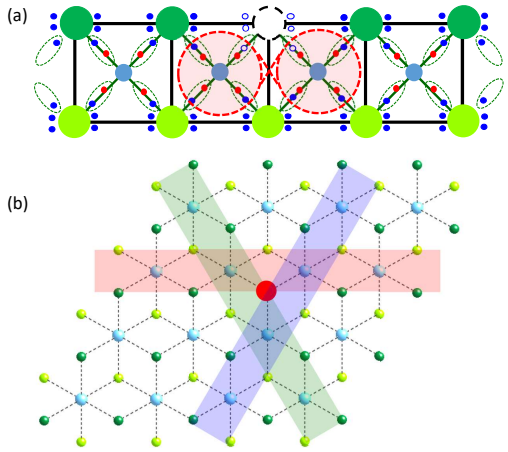

Fig. 7 (a) The proposed valence bond model for localized electrons/holes generated as a result of Se vacancies. (b) For each Se vacancy center, there are actually three equivalent routes for the localized electrons/holes with preserved C_3 symmetry within each tri-atomic layer, as illustrated by the three equivalent stripes viewed along c-direction.

$2a$ periodicity along one of the three equivalent chain directions in each layer, as illustrated in Figs. 2(b) and 7(b). Due to the multiple types of defect that can intercalate into the vdW gaps and introduce doped carriers, domains of various sizes and chain directions are expected to be found.[34] Within each domain of specific chain orientation, the chain direction of its neighboring layers is expected to pick a different orientation to reduce the inter-layer Coulomb repulsion but maintain strong vdW force via electric dipoles across the vdW gap. Although the choice of chain direction in the neighboring layer is random under quantum fluctuation, i.e., either clockwise or counter-clockwise, additional chiral symmetry breaking for charge along the c-direction must be responsible for the observed $2c$ periodicity.

Among the defects that can be used as pinning centers for the chiral CDW, we propose that the Se vacancy is the most effective, as illustrated in Fig. 7(a). Once an edge Se atom is removed from the $TiSe_2$-ribbon, the electrons in the dangling bonds of Ti become unstable, resulting in a slight increase in energy above the Fermi level, with partial localization near the Se vacancy center of unpaired electrons achieved via electron sharing with the neighboring valence electrons in the σ-bond or Se lone pairs. In fact, significant amounts of Se vacancies of $\delta\sim$0.08 - 0.17 have been identified in $1T$-$TiSe_{2-\delta}$ prepared under various temperature and annealing conditions.[17] Based on resistivity ρ(T) measurement results, the band picture changes as a function of δ to show evolution of the transport property from being semiconducting-like for $\delta\sim$0.08 to metallic-like up to $\delta\sim$0.17. Among the inconsistent physical properties of samples reported in the literature, the sample with $\delta\sim$0.12 is found to show the most pronounced 2a*2a*2c CDW phase below $\sim$200 K, unfortunately it has often been misidentified to be stoichiometric in the absence of chemical analysis.[9] While the optimal 2a*2a*2c CDW phase has always been found in samples of $\delta\sim0.12\approx1/8$, it is suggested that on average, one in eight formula units contain an Se vacancy, which naturally leads to an intra-layer 2a*2a periodicity and the inter-layer $2c$ periodicity.

Starting from the TiSe2-ribbon construction in the (0 0 1) projection view, as shown in Fig. 7(b), it is found that whenever a localized charge is pinned near the Se vacancy center,[35] three equivalent choices are possible for the chain directions of a $TiSe_2$-ribbon. For a condensed matter trying to reach its true ground state, additional chirality symmetry breaking may have occurred based on the observed chiral CDW by Ishioka *et al.*, where a fixed chirality of clockwise or counter-clockwise handedness indicates additional charge ordering along the c-direction. Since a chiral CDW was observed in different areas of the sample studied by Ishioka *et al.*,[34] which showed a pronounced 2a*2a*2c CDW phase as well, we suggest that both the 2a*2a*2c and chiral CDW phases are of the same origin as a result of Se vacancy-induced self-doping, especially for samples of Se vacancy level $\delta\sim$0.12 showing the most pronounced 2a*2a*2c resistivity anomaly.

4 Conclusions

In summary, we have proposed a valence bond model for the prototypical TMDC vdW material $1T$-$TiSe_2$, which contains a tri-atomic layer as a quasi-2D system. The four valence electrons per Ti atom and the four neighboring Se atoms per square plaquette satisfy the Ti-dsp^2 hybridized orbitals to form σ-bonds in the $TiSe_2$-ribbon plane. dp type π-bond formation among empty Ti-$3d_{yz}/3d_{zx}$ orbitals and the lone pair of Se-$4p_z$ is proposed and supported by the collective plasmonic resonance detected by the EELS spectrum. Current findings must contribute to the TMDC research in four aspects: to the understanding of its controversial CDW phase, the ribbon stripe view of $1T$-$TiSe_2$ and its chiral nature explains the observed chiral CDW reasonably; to the potential device application using 1D and 2D transport character, the conjugated 1D π-bond system with 2D chiral nature could inspire the development of novel tuning mechanisms; to the advancement of 2D mono to few-layer research, the newly identified conjugated π-bond system bridges TMDC layered materials to the recent topological materials unexpectedly and worth to explore further; and to the research of defect physics and chemistry, it is implied that the role of vacancy defect in TMDC materials should be re-examined more carefully from the end of material preparation to the electric property interpretations.

Conflicts of interest

There are no conflicts to declare.

Acknowledgements

FCC acknowledges the support provided by the Ministry of Science and Technology in Taiwan under project number MOST-106-2119-M-002-035-MY3. GJS acknowledges the support provided by MOST-Taiwan under project number 105-2112-M-027-003-MY3. This work was also financially supported by the Center of Atomic Initiative for New Materials, National Taiwan University, Taipei 10617, Taiwan from the Featured Areas Research Center Program within the framework of the Higher Education Sprout Project by the Ministry of Education (MOE) in Taiwan.

Notes and references

1 A. H. Castro Neto, F. Guinea, N. M. R. Peres, K. S. Novoselov and A. K. Geim, *Rev. Mod. Phys.*, 2009, **81**, 109.

2 S. J. McDonnell and R. M. Wallace, *Thin Solid Films*, 2016, **616**, 482–501.

3 H. Zheng, S. Valtierra, N. Ofori-Opoku, C. Chen, L. Sun, S. Yuan, L. Jiao, K. H. Bevan and C. Tao, *Nano Letters*, 2018, **18**, 2179–2185.

4 F. A. Lévy, *Crystallography and crystal chemistry of materials with layered structures*, Springer Science & Business Media, 2012, vol. 2.

5 F. D. M. Haldane, *Reviews of Modern Physics*, 2017, **89**, 040502.

6 R. Sankar, G. Narsinga Rao, I. P. Muthuselvam, C. Butler, N. Kumar, G. Senthil Murugan, C. Shekhar, T.-R. Chang, C.-Y. Wen, C.-W. Chen *et al.*, *Chemistry of Materials*, 2017, **29**, 699–707.

7 X. Qian, J. Liu, L. Fu and L. J, *Science*, 2014, **346**, 1344.

8 J. A. Wilson, *physica status solidi (b)*, 1978, **86**, 11–36.

9 F. J. Di Salvo and J. V. Waszczak, *Physical Review B*, 1978, **17**, 3801.

10 J. C. E. Rasch, T. Stemmler, B. Müller, L. Dudy and M. R, *Phys. Rev. Lett.*, 2008, **101**, 237602.

11 B. Hildebrand, C. Didiot, A. M. Novello, G. Monney, A. Scarfato, A. Ubaldini, H. Berger, D. Bowler, C. Renner and P. Aebi, *Physical review letters*, 2014, **112**, 197001.

12 G. J. Shu and F. C. Chou, *Physical Review B*, 2013, **88**, 155130.

13 G. J. Shu, S. C. Liou, S. K. Karna, R. Sankar, M. Hayashi and F. C. Chou, *Physical Review Materials*, 2018, **2**, 044201.

14 G. J. Shu, S. C. Liou, S. K. Karna, R. Sankar, M. Hayashi, M.-W. Chu and F. C. Chou, *Applied Physics Letters*, 2015, **106**, 122101.

15 M. Imada, A. Fujimori and Y. Tokura, *Reviews of modern physics*, 1998, **70**, 1039.

16 M. Z. Hasan and C. L. Kane, *Rev. Mod. Phys.*, 2010, **82**, 3045.

17 S. H. Huang, G. J. Shu, W. W. Pai, H. L. Liu and F. C. Chou, *Physical Review B*, 2017, **95**, 045310.

18 C. Riekel, *Journal of Solid State Chemistry France*, 1976, **17**, 389–392.

19 G. J. Shu and F. C. Chou, *Physical Review B*, 2016, **93**, 140402.

20 J. van Wezel, P. Nahai-Williamson and S. Saxena, *physica status solidi (b)*, 2010, **247**, 592–594.

21 J. van Wezel, P. Nahai-Williamson and S. S. Saxena, *Physical Review B*, 2010, **81**, 165109.

22 H. Raether, *Excitation of plasmons and interband transitions by electrons*, Springer, 2006, vol. 88.

23 R. F. Egerton, *Electron energy-loss spectroscopy in the electron microscope*, 2011.

24 A. Politano, V. L and M. S. Vitiello, *APL Mater.*, 2017, **5**, 035504.

25 A. Politano, G. Chiarello, C. N. Kuo, C.-S. Lue, R. Edla, P. Torelli, V. Pellegrini and D. W. Boukhvalov, *Advanced Functional Materials*, 2018, **28**, 1706504.

26 A. Politano, G. Chiarello, B. Ghosh, K. Sadhukhan, C. N. Kuo, C.-S. Lue, V. Pellegrini and A. Agarwal, *Physical Review Letters*, 2018, **121**, 086804.

27 A. Agarwal, M. S. Vitiello, L. Viti, A. Cupolillo and A. Politano, *Nanoscale*, 2018, **10**, 8938–8946.

28 L. Viti, D. Coquillat, A. Politano, K. A. Kokh, Z. S. Aliev, M. B. Babanly, O. E. Tereshchenko, W. Knap, E. V. Chulkov and M. S. Vitiello, *Nano Letters*, 2015, **16**, 80–87.

29 S. C. Liou, M.-W. Chu, R. Sankar, F.-T. Huang, G. J. Shu, F. C. Chou and C. H. Chen, *Physical Review B*, 2013, **87**, 085126.

30 A. Politano, V. M. Silkin, I. A. Nechaev, M. S. Vitiello, L. Viti, Z. S. Aliev, M. B. Babanly, G. Chiarello, P. M. Echenique and E. V. Chulkov, *Physical Review Letters*, 2015, **115**, 216802.

31 A. Politano, G. Chiarello and C. Spinella, *Materials Science in Semiconductor Processing*, 2017, **65**, 88–99.

32 I. Affleck, T. Kennedy, L. E. H and T. H, *Phys. Rev. Lett.*, 1987, **59**, 799.

33 P. Aebi, T. Pillo, H. Berger and F. Lévy, *Journal of electron spectroscopy and related phenomena*, 2001, **117**, 433–449.

34 J. Ishioka, Y. H. Liu, K. Shimatake, T. Kurosawa, K. Ichimura, Y. Toda, M. Oda and S. Tanda, *Phys. Rev. Lett.*, 2010, **105**, 176401–4.

35 H. H. Weitering, J. M. Carpinelli, A. V. Melechko, J. Zhang, M. Bartkowiak and E. W. Plummer, *Science*, 1999, **285**, 2107–2110.